arXiv:0809.2718v1 [cond-mat.mes-hall] 16 Sep 2008

Resonant circular photogalvanic effect in GaN/AlGaN heterojunctions

B. Wittmann,[1] L. E. Golub,[2] S. N. Danilov,[1] J. Karch,[1] C. Reitmaier,[1] Z. D. Kvon,[3]
N. Q. Vinh,[4] A. F. G. van der Meer,[4] B. Murdin,[5] and S. D. Ganichev[1]*
[1] *Terahertz Center, University of Regensburg, 93040 Regensburg, Germany*
[2] *A.F. Ioffe Physico-Technical Institute, Russian Academy of Sciences, 194021 St. Petersburg, Russia*
[3] *Institute of Semiconductor Physics, Russian Academy of Sciences, 630090 Novosibirsk, Russia*
[4] *FOM Institute for Plasma Physics "Rijnhuizen", P.O. Box 1207, NL-3430 BE Nieuwegein, The Netherlands and*
[5] *University of Surrey, Guildford, GU2 7XH, UK*
(Dated: February 10, 2022)

The resonant circular photogalvanic effect is observed in wurtzite (0001)-oriented GaN low-dimensional structures excited by infrared radiation. The current is induced by angular momentum transfer of photons to the photoexcited electrons at resonant inter-subband optical transitions in a GaN/AlGaN heterojunction. The signal reverses upon the reversal of the radiation helicity or, at fixed helicity, when the propagation direction of the photons is reversed. Making use of the tunability of the free-electron laser FELIX we demonstrate that the current direction changes by sweeping the photon energy through the intersubband resonance condition, in agreement with theoretical considerations.

PACS numbers: 73.21.Fg, 78.67.De, 73.63.Hs, 72.25.Dc

I. INTRODUCTION

Wide bandgap GaN has been extensively investigated for applications as blue and ultraviolet light sources[1] as well as for high temperature and high power electronic devices.[2,3,4] The commercial fabrication of blue and green LEDs has led to well established technological procedures of epitaxial GaN preparation and sparked a great research activity on the properties of heterostructures based on GaN and its alloys with AlN and InN. Most recently two-dimensional GaN attracted growing attention as a potentially interesting material system for semiconductor spintronics since, doped with manganese, it is expected to become ferromagnetic with a Curie-temperature above room temperature,[5] gadolinium doped it may offer an opportunity for fabricating magnetic semiconductors,[6,7,8,9] and since GaN-based structures show long spin relaxation times[10] and considerable Rashba spin splitting[11] due to strong built-in electric fields. First indications of substantial spin-orbit splitting came from the observation of the circular photogalvanic effect (CPGE)[12,13] in GaN heterojunctions at Drude absorption of THz radiation[14] and was then confirmed by magneto-transport measurements yielding a value for the Rashba splitting of about 0.3 meV at the Fermi wavevector.[15,16,17] Making use of interband absorption, the investigations of the CPGE were extended to GaN quantum wells as well as to low dimensional structures under uniaxial strain, confirming the Rashba character of the spin splitting.[18,19,20]

In this paper we report on the observation of the resonant CPGE due to inter-subband transitions and present the phenomenological theory as well as the microscopic model of this phenomenon. We demonstrate that variation of the photon energy in the vicinity of the resonance results in a change of sign of the photocurrent. This proves the dominant contribution to the total current from the asymmetry in momentum distribution of carriers excited in optical transitions. We analyze spin-dependent as well as spin-independent mechanisms giving rise to a resonant photocurrent and demonstrate that, in spite of the weak spin-orbit interaction, the resonant CPGE in GaN is mostly caused by the spin-dependent mechanism.

II. SAMPLES AND EXPERIMENTAL METHODS

Experiments were carried out on GaN/$Al_{0.3}Ga_{0.7}N$ heterojunctions grown by MOCVD on C(0001)-plane sapphire substrates (for details of growth see Ref. 14). The thickness of the AlGaN layers was varied between 30 nm and 100 nm. An undoped 33 nm thick GaN buffer layer grown under a pressure of 40 Pa at temperature 550°C is followed by an undoped GaN layer (~ 2.5 μm) grown under 40 Pa at 1025°C; the undoped $Al_{0.3}Ga_{0.7}N$ barrier was grown under 6.7 Pa at 1035°C. The mobility and density in the two-dimensional electron gas measured at room temperature are $\mu \approx 1200$ cm^2/Vs and $N_e \approx 10^{13}$ cm^{-2}, respectively. To measure the photocurrent two pairs of contacts are centered at opposite sample edges with the connecting lines along the axes $x \parallel [11\bar{2}0]$ and $y \parallel [\bar{1}100]$, see inset in the top of Fig. 1. In order to excite resonantly transitions between the size quantized subbands $e1$ and $e2$ and to obtain a measurable photocurrent it was necessary to have a tunable high power radiation source for which we used the free electron laser "FELIX" at FOM-Rijnhuizen in the Netherlands oper-

*e-mail: sergey.ganichev@physik.uni-regensburg.de

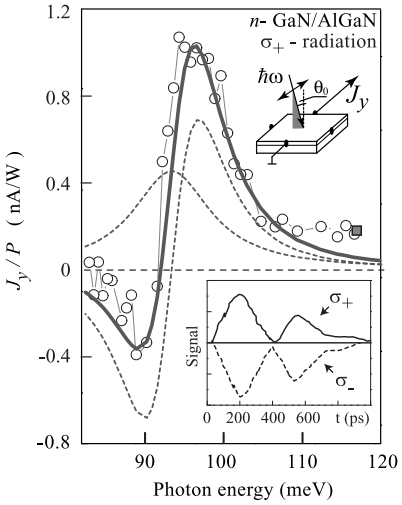


FIG. 1: Spectral dependence of the transversal photocurrent J_y measured at room temperature at oblique incidence ($\theta_0 = 15^\circ$) for right-handed circularly polarized radiation. The data are obtained by the free electron laser FELIX (dots) and TEA CO_2 laser (square). The radiation power used for these measurements was about 35 kW for the CO_2 laser and about 100 kW for FELIX. The magnitude of the current measured at FELIX is fit at this plot to that obtained with the CO_2 laser, assuming that the current depends linearly on the radiation power at used power level. The solid line represents a fit by the sum of asymmetrical and symmetrical contributions to Eq. (2). The inset in the bottom corner shows the temporal structure of the current in response to the radiation of FELIX. The inset in the upper corner demonstrates the experimental geometry.

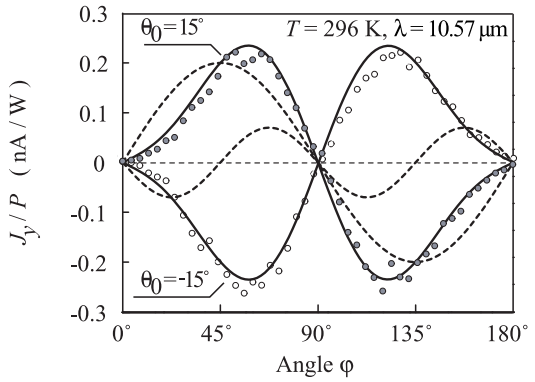


FIG. 2: Photocurrent as a function of the angle φ measured at oblique incidence ($\theta_0 = \pm 15^\circ$) in the transverse geometry. The data are obtained in close circuit configuration applying TEA CO_2 laser operating at a wavelength $\lambda = 10.57$ μm and a power $P \approx 35$ kW. Solid lines are fits of the photocurrent to Eq. (1) at $\gamma/\chi = 1.4$. The two contributions to Eq. (1) are shown by dashed lines for $\theta_0 = 15^\circ$.

ating in the spectral range between 8 μm and 15 μm.[21] The output pulses of light from FELIX were chosen to be about 3 ps long, separated by 40 ns, in a train (or "macropulse") of duration of 7 μs. The macropulses had a repetition rate of 5 Hz. The linearly polarized light from FELIX was converted into left handed (σ_-) and right handed (σ_+) circularly polarized radiation by means of a Fresnel rhomb. A rotation of the optical axis of the Fresnel rhomb's plate by an angle φ with respect to the laser radiation polarization plane results in a variation of the radiation helicity as $P_{\rm circ} = \sin 2\varphi$. Here the angle $\varphi = 0$ corresponds to the setting where the position of the polarizer optical axis coincides with the incoming laser polarization. Radiation is applied at oblique incidence described by an angle of incidence θ_0 varying from -15° to $+15^\circ$, see the top inset to Fig. 1.

III. EXPERIMENTAL RESULTS AND PHENOMENOLOGICAL DESCRIPTION

On illumination of the low-dimensional structures by circularly polarized radiation at room temperature at oblique incidence in (xz)-plane we observe a current signal in the y direction perpendicular to the plane of incidence, Fig. 1. The current reverses its direction by switching the sign of the radiation helicity. Signals in response to the left handed and right handed polarized radiation are shown in the lower inset of Fig. 1. Using short 3 ps pulses of FELIX we observed that the response time was determined by the time resolution of our set-up which therefore sets an upper limit to the response time. This fast response is typical for photogalvanics, where the signal decay time is expected to be of the order of the momentum relaxation time[12,13,22] being in our samples at room temperature typically about 0.1 ps. Figure 2 demonstrates the dependences of the photocurrent on the angle φ for two angles of incidence $\theta_0 = \pm 15^\circ$. The photocurrent signals generated in the unbiased devices were measured via an amplifier with a response time of the order of 1 μs, i.e. averaged over the macropulse. The current closely follows the radiation helicity $P_{\rm circ} = \sin 2\varphi$. The signal proportional to the helicity is only observed under oblique incidence. The current vanishes for normal incidence and changes its polarity when the incidence angle changes its sign, see Fig. 2. The photocurrent in the layer flows always perpendicularly to the direction of the incident light propagation and its magnitude does not change by rotating the sample around the growth axis.

Investigating the spectral dependence of the photocurrent we observe that for both, left and right handed circular polarizations, the current changes sign at a photon energy $\hbar\omega \approx 93$ meV, see Fig. 1. Figure 1 also shows that the spectral behaviour of the current can be well described by the sum of the derivative of the Lorentzian-like absorption spectrum and an additional contribution proportional to the absorption spectrum itself.

A phenomenological analysis for the C_{3v} point group symmetry relevant to the structures under study shows that the φ-dependence of the transverse photogalvanic current density $\boldsymbol{j}$ under excitation at oblique incidence

in (xz)-plane is given by[14,23]

$$j_y(\varphi) = E_0^2 t_p t_s \sin\theta \left(\gamma \sin 2\varphi - \frac{\chi}{2} \sin 4\varphi\right). \qquad (1)$$

Here E_0 is the amplitude of the electromagnetic wave, θ is the refraction angle related to the incidence angle θ_0 by $\sin\theta = \sin\theta_0/n_\omega$, where n_ω is the refractive index, and t_s and t_p are the Fresnel amplitude transmission coefficients from vacuum to the structure for the s- and p-polarized light, respectively.[24] The coefficient γ is a component of the second-rank pseudotensor $\boldsymbol{\gamma}$ which describes the helicity dependent current, comprising the CPGE and the optically induced spin-galvanic effect,[25] and χ is a component of the third-rank tensor $\boldsymbol{\chi}$ describing the linear photogalvanic effect.[12,13,23] In systems of C_{3v} symmetry the tensor $\boldsymbol{\gamma}$ has one linearly-independent component, namely $\gamma_{xy} = -\gamma_{yx} \equiv \gamma$. Thus, the CPGE current flows always perpendicularly to the plane of incidence. The components of the tensor $\boldsymbol{\chi}$ are given by $\chi \equiv \chi_{xxz} = \chi_{yyz}$, where $z \parallel [0001]$ is the C_3 axis. We take into account that the second linearly-independent component of $\boldsymbol{\chi}$ in C_{3v} systems is much smaller than χ, so that the corresponding photocurrent is negligible at oblique incidence.[23]

The fits of the experiment to Eq. (1) at $\gamma/\chi = 1.4$ are shown in Fig. 2 for $\theta_0 = \pm 15^\circ$ by solid lines demonstrating a good agreement with the experimental data. Figure 2 shows that the dominant contribution to the photocurrent is due to the helicity dependent current given by the first term on the right-hand side of the Eq. (1). The fact that the magnitude of the photocurrent does not change by rotating the sample around the growth axis is in agreement with the fact that in structures of C_{3v} symmetry the tensor $\boldsymbol{\gamma}$ has one linearly-independent component.

IV. MICROSCOPIC MODELS AND DISCUSSION

Two microscopic mechanisms are known to give rise to helicity-dependent currents exhibiting sign reversal for photon energies matching the energy separation between size-quantized subbands. The first is caused by an asymmetry of the momentum distribution of carriers excited by direct optical transitions in the system with the Rashba splitting of energy subbands.[12,13] Spectral inversion at resonance is a characteristic feature of this CPGE mechanism and has also been observed in GaAs QWs.[26,27] The second mechanism is of orbital nature and spin-independent. It is caused by the quantum mechanical interference of various pathways in Drude absorption.[28] This effect has most recently been demonstrated in Si-MOSFET inversion layers, where spin dependent mechanisms are absent due to vanishingly small spin-orbit interaction in silicon.[29] The spectral inversion in orbital mechanism is caused by a difference of the virtual states in the excited subband needed for the pathway

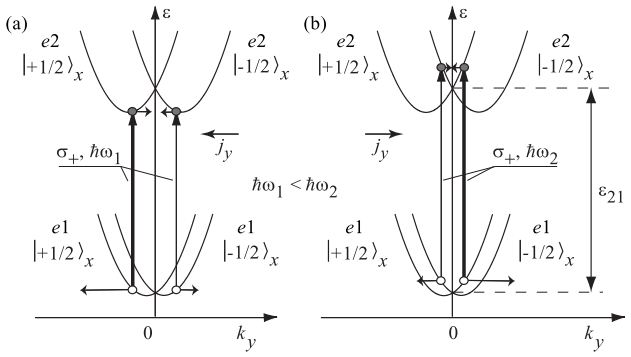


FIG. 3: Microscopic picture describing the origin of the CPGE and its spectral sign inversion in C_{3v} point group samples. (a) Excitation at oblique incidence with σ_+ radiation of $\hbar\omega$ less than the subband energy separation ε_{21} induces direct spin-conserving transitions (vertical arrows). The rates of these transitions are different as illustrated by the different thickness of the arrows (reversing the angle of incidence mirrors the thickness of the arrows). This leads to a photocurrent due to an asymmetrical distribution of carriers in $\boldsymbol{k}$-space if the splitting of the $e1$ and $e2$ subbands are not equal. (b) Increasing of the photon energy shifts more intensive transitions to the right and less intensive to the left, resulting in a change of the photocurrent sign.

with direct virtual optical transitions. Below we consider both mechanisms and compare their contributions to the total photocurrent.

The spin-dependent mechanism of the CPGE caused by direct inter-subband transitions at oblique incidence is illustrated in Fig. 3 for σ_+ radiation. In C_{3v} symmetry the $\alpha\sigma_x k_y$ term in the Rashba Hamiltonian splits the subbands in the k_y direction into two spin branches with the spin projection $\pm 1/2$ oriented along x. Due to selection rules, like in (001)-grown GaAs QWs of C_{2v} symmetry, the absorption of circularly polarized radiation is spin-conserving.[26] It turns out, however, that under oblique excitation with circularly polarized light the rates of inter-subband transitions are different for electrons with the spin oriented parallel and antiparallel to the in-plane direction of light propagation.[26] This is depicted in Fig. 3 by vertical arrows of different thickness. In systems with $\boldsymbol{k}$-linear spin splitting such processes lead to an asymmetrical distribution of carriers in $\boldsymbol{k}$-space, i.e. to an electrical current. The inversion of photon helicity driven current is a direct consequence of $\boldsymbol{k}$-linear terms in the band structure of subbands together with energy and momentum conservation as well as optical selection rules for direct optical transitions between size quantized subbands. At photon energy $\hbar\omega_1 < \varepsilon_{21}$ of right circularly polarized radiation the most intense optical transition occurs at negative k_y resulting in a current j_y shown by an arrow in Fig. 3 (a). Here ε_{21} is the intersubband energy separation. Increase of the photon energy shifts the transition toward positive k_y and reverses the direction of the current, see Fig. 3 (b). In the frame of this model the sign reversal of the current takes place at the

photon energy $\hbar\omega = \varepsilon_{21}$ corresponding to optical transitions from the band minima. The CPGE current at direct inter-subband transitions is given by[26]

$$j_{\rm spin} = \Lambda(\alpha_1-\alpha_2)\frac{e}{\hbar}\frac{IP_{\rm circ}}{\hbar\omega} \times\left[(\tau_p^{(1)}-\tau_p^{(2)})\bar{E}\frac{d\eta_{21}(\hbar\omega)}{d\hbar\omega}+\tau_p^{(2)}\eta_{21}(\hbar\omega)\right]. \quad (2)$$

Here $\alpha_{1,2}$ are the Rashba constants for electrons in the first and second subbands, the factor Λ describes monopolar spin orientation of carriers under resonant transitions, $\tau_p^{(1)}$ and $\tau_p^{(2)}$ are the momentum relaxation times in the initial and final state of optical transition, $\bar{E}$ is the average kinetic energy of carriers, $\eta_{21}(\hbar\omega)$ is the intersubband absorbance which in the model of an infinitely-deep rectangular quantum well is given by[12]

$$\eta_{21}(\hbar\omega) = \frac{512}{27\pi}\frac{N_e e^2\hbar}{cmn_\omega}\frac{\Gamma}{(\varepsilon_{21}-\hbar\omega)^2+\Gamma^2},$$

where m is the electron effective mass and Γ is the peak width. The 2DEG in GaN structures is almost degenerate even at room temperature due to the large Fermi energy: $\bar{E} \approx 100$ meV $> k_{\rm B}T$. Therefore, in contrast to GaAs based structures, the optical phonon emission by photoexcited electrons in the $e2$ subband is suppressed (also due to the high frequency of the optical phonon in GaN). As a result, both initial and final states have momentum relaxation times of the same order, so that both symmetrical [$\propto \eta_{21}(\hbar\omega)$] and asymmetrical [$\propto d\eta_{21}/d(\hbar\omega)$] terms give comparable contributions to the CPGE. This is due to the fact that GaN based low dimensional structures have a large energy of optical phonons and typically a rather large Fermi energy compared to the GaAs QWs.

The orbital mechanism of the CPGE is caused by Drude like absorption which is usually rather small at infrared frequencies used in the experiment. However, its contribution to the total photocurrent may be comparable with the spin-dependent mechanism and, therefore, should be analyzed. Following Refs. 28,29 the orbital mechanism of the CPGE is described by

$$j_{\rm orb} = \xi z_{21}\frac{4\pi\kappa e^3 N_e}{\omega cmn_\omega}\frac{\varepsilon_{21}}{\varepsilon_{21}^2-(\hbar\omega)^2}IP_{\rm circ}, \quad (3)$$

where ξ is the factor of scattering asymmetry, and $\kappa \gtrsim 1$.[28] This equation shows that the CPGE due to the orbital mechanism also changes the photocurrent sign for photon energies matching the energy separation.

To compare spin-dependent and orbital contributions to the CPGE we take magnitudes of the photocurrent at the wings of the absorption contour ($|\hbar\omega-\varepsilon_{21}|=\Gamma$). Equations (2) and (3) give an estimate for the ratio of the contributions as

$$j_{\rm spin}/j_{\rm orb} \sim \frac{\Lambda}{\xi}\frac{(\alpha_1-\alpha_2)\omega\tau_p^{(1)}}{\Gamma z_{21}}\frac{\bar{E}}{\varepsilon_{21}}.$$

The factor Λ describing monopolar spin orientation of carriers under resonant transitions with account for both crystal (Δ_{cr}) and spin-orbit (Δ) splittings of the valence band provided $\Delta \ll \Delta_{cr} \ll E_g$ (E_g is the fundamental energy gap) is given by

$$\Lambda = \frac{\varepsilon_{21}\,\Delta}{3E_g^2}.$$

It can be estimated for investigated GaN based structures as $\Lambda \sim 0.03$. This substantially smaller value of Λ in GaN structures compared to GaAs QWs is caused by a small spin-orbit interaction in the nitrogen atom, yielding $\Delta/E_g \approx 10^{-3}$ for GaN. Taking $\varepsilon_{21} = 100$ meV and $\Gamma = 6$ meV from the photocurrent spectrum, $z_{21} = 10$ Å,[30] $|\alpha_1-\alpha_2| \sim \alpha_1 \approx 10^{-10}$ eV cm,[15,16] and $\xi = 10^{-2}$ as in Ref. 29, we obtain that the spin-dependent contribution to CPGE caused by resonant direct transitions is about five times larger than the CPGE due to the orbital mechanism caused by quantum interference in Drude absorption.

This conclusion is also supported by the shape of the CPGE spectrum. Indeed, Fig. 1 shows that the shape of the spectrum is substantially asymmetric. The orbital mechanism described by Eq. (3) yields only a slight asymmetry while for the spin-dependent mechanism in GaN structures we obtain that the photocurrent is a superposition of comparable symmetric [$\propto \eta_{21}(\hbar\omega)$] and asymmetric [$\propto d\eta_{21}/d(\hbar\omega)$] parts, Eq. (2). Figure 1 shows that Eq. (2) describes well the whole spectral behaviour. We note that, when considering the spin dependent contribution to the helicity dependent photocurrent, one should also take into account a possible admixture of the spin-galvanic effect which is proportional to the radiation absorbance and $P_{\rm circ}$. The interplay between CPGE and the spin-galvanic effect caused by resonant inter-subband transitions has been reported for GaAs QWs.[27]

To summarize, we demonstrate that in GaN low dimensional structures resonant intersubband transitions result in a circular photogalvanic effect with a dominant contribution by the spin dependent mechanism. The specific feature of the resonant CPGE in GaN heterojunctions is that the symmetric and asymmetric components of the photocurrent have comparable strengths.

Acknowledgments

We thank E.L. Ivchenko, V.V. Bel'kov and S.A. Tarasenko for their permanent interest in this activity and the many discussions that helped to clarify the problem under study. The financial support from the DFG and RFBR is gratefully acknowledged. Work of L.E.G. is also supported by "Dynasty" Foundation — ICFPM and President grant for young scientists. The high quality GaN samples were kindly provided by Hyun-Ick Cho and Jung-Hee Lee from Kyungpook National University, Korea.

[1] S. Nakamura, S. Pearton, and G. Fasol, *The Blue Laser Diode. The Complete Story* (Springer, Berlin, 2007).

[2] Q. Chen, M. Asif Khan, J. W. Yang, C. J. Sun, M. S. Shur, and H. Park, Appl. Phys. Lett. **69**, 794 (1996).

[3] Y.-F. Wu, B. P. Keller, S. Keller, D. Kapolnek, P. Kozodoy, S. P. Denbaars, and U. K. Mishra, Appl. Phys. Lett. **69**, 1438 (1996).

[4] O. Ambacher, J. Smart, J. R. Shealy, N. G. Weimann, K. Chu, M. Murphy, W. J. Schaff, L. F. Eastman, R. Dimitrov, L. Wittmer, M. Stutzmann, W. Rieger, and J. Hilsenbeck, J. Appl. Phys. **85**, 3222 (1999).

[5] T. Dietl, H. Ohno, F. Matsukura, J. Cibert, and D. Ferrand, Science **287**, 1019 (2000).

[6] S. Dhar, O. Brandt, M. Ramsteiner, V. F. Sapega, and K. H. Ploog, Phys. Rev. Lett. **94**, 037205 (2005).

[7] G. M. Dalpian, S. H. Wei, Phys. Rev. B **72**, 115201 (2005).

[8] S. Dhar, T. Kammermeier, A. Ney, L. Prez, K. H. Ploog, A. Melnikov, and A. D. Wieck, Appl. Phys. Lett. **89**, 062503 (2006).

[9] M. A. Khaderbad, S. Dhar, L. Prez, K. H. Ploog, A. Melnikov, and A. D. Wieck, Appl. Phys. Lett. **91**, 072514 (2007).

[10] B. Beschoten, E. Johnston-Halperin, D. K. Young, M. Poggio, J. E. Grimaldi, S. Keller, S. P. DenBaars, U. K. Mishra, E. L. Hu, and D. D. Awschalom, Phys. Rev. B **63**, 121202(R) (2001).

[11] Yu. A. Bychkov and E. I. Rashba, Pis'ma Zh. Eksp. Teor. Fiz. **39**, 66 (1984) [JETP Lett. **39**, 78 (1984)].

[12] E. L. Ivchenko, *Optical Spectroscopy of Semiconductor Nanostructures* (Alpha Science International, Harrow, UK, 2005).

[13] S. D. Ganichev and W. Prettl, *Intense Terahertz Excitation of Semiconductors* (Oxford University Press, Oxford, 2006).

[14] W. Weber, S. D. Ganichev, Z. D. Kvon, V. V. Bel'kov, L. E. Golub, S. N. Danilov, D. Weiss, W. Prettl, Hyun-Ick Cho, and Jung-Hee Lee, Appl. Phys. Lett. **87**, 262106 (2005).

[15] N. Thillosen, Th. Schäpers, N. Kaluza, H. Hardtdegen, and V. A. Guzenko, Appl. Phys. Lett. **88**, 022111 (2006).

[16] S. Schmult, M. J. Manfra, A. Punnoose, A. M. Sergent, K. W. Baldwin, and R. J. Molnar, Phys. Rev. B **74**, 033302 (2006).

[17] N. Tang, B. Shen, M. J. Wang, K. Han, Z. J. Yang, K. Xu, G. Y. Zhang, T. Lin, B. Zhu, W. Z. Zhou, and J. H. Chu, Appl. Phys. Lett. **88**, 172112 (2006).

[18] X. W. He, B. Shen, Y. Q. Tang, N. Tang, C. M. Yin, F. J. Xu, Z. J. Yang, G. Y. Zhang, Y. H. Chen, C. G. Tang, and Z. G. Wang, Appl. Phys. Lett. **91**, 071912 (2007).

[19] Y. Q. Tang, B. Shen, X. W. He, K. Han, N. Tang, W. H. Chen, Z. J. Yang, G. Y. Zhang, Y. H. Chen, C. G. Tang, Z. G. Wang, K. S. Cho, and Y. F. Chen, Appl. Phys. Lett. **91**, 071920 (2007).

[20] K. S. Cho, C.-T. Liang, Y. F. Chen, Y. Q. Tang, and B. Shen, Phys. Rev. B **75**, 085327 (2007).

[21] G. M. H. Knippels, X. Yan, A. M. MacLeod, W. A. Gillespie, M. Yasumoto, D. Oepts, and A. F. G. van der Meer, Phys. Rev. Lett. **83**, 1578 (1999).

[22] B. I. Sturman and V. M. Fridkin, *The Photovoltaic and Photorefractive Effects in Non-Centrosymmetric Materials* (Gordon and Breach, New York, 1992).

[23] W. Weber, L. E. Golub, S. N. Danilov, J. Karch, C. Reitmaier, B. Wittmann, V. V. Bel'kov, E. L. Ivchenko, Z. D. Kvon, N. Q. Vinh, A. F. G. van der Meer, B. Murdin, and S. D. Ganichev, Phys. Rev. B **77**, 245304 (2008)

[24] M. Born and E. Wolf, *Principles of Optics* (Pergamon Press, Oxford, 1970).

[25] S. D. Ganichev, E. L. Ivchenko, V. V. Bel'kov, S. A. Tarasenko, M. Sollinger, D. Weiss, W. Wegscheider, and W. Prettl, Nature (London) **417**, 153 (2002).

[26] S. D. Ganichev, V. V. Belkov, Petra Schneider, E. L. Ivchenko,S. A. Tarasenko, W. Wegscheider, D. Weiss, D. Schuh, E. V. Beregulin, and W. Prettl, Phys. Rev. B **68**, 035319 (2003).

[27] S. D. Ganichev, Petra Schneider, V. V. Belkov, E. L. Ivchenko, S. A. Tarasenko, W. Wegscheider, D. Weiss, D. Schuh, B. N. Murdin, P. J. Phillips, C. R. Pidgeon, D. G. Clarke, M. Merrick, P. Murzyn, E. V. Beregulin, and W. Prettl, Phys. Rev. B **68**, 081302(R) (2003).

[28] S. A. Tarasenko, Pis'ma Zh. Eksp. Teor. Fiz. **85**, 216 (2007) [JETP Lett. **85**, 182 (2007)].

[29] P. Olbrich, S. A. Tarasenko, C. Reitmaier, J. Karch, D. Plohmann, Z. D. Kvon, S.D. Ganichev, arXiv:0808.1987v1 (2008).

[30] V. I. Litvinov, Phys. Rev. B **68**, 155314 (2003).